ISSN (Print) 1226-1750
ISSN (Online) 2233-6656
Journal of Magnetics 19(4), 323-326 (2014) http://dx.doi.org/10.4283/JMAG.2014.19.4.323

Preparation and Physical Characterizations of Superparamagnetic Maghemite Nanoparticles

Sunghyun Yoon*

Department of Physics, Gunsan National University, Gunsan 573-701, Korea

(Received 19 August 2014, Received in final form 19 September 2014, Accepted 22 September 2014)

Superparamagnetic maghemite nanoparticles were prepared by chemical co-precipitation, followed by a temperate oxidation stage, and investigated using FE-SEM, XRD, TGA, VSM, and Mössbauer spectroscopy. Through SEM image and XRD analysis, its average particle size was found to be 13.9 nm. While VSM magnetic measurement showed typical superparamagnetic behavior at room temperature, Mössbauer spectroscopic investigation revealed that non-vanishing magnetic hyperfine structure were retained. Cation distribution estimated from Mössbauer spectroscopy confirmed the formation of maghemite nanophase in the sample.

Keywords : superparamagnetism, maghemite nanoparticles, cation distribution, Mössbauer spectroscopy

1. Introduction

Magnetic properties of nano-sized particles have been of great importance in fields ranging from pure scientific through biomedical to technological and industrial applications [1, 2]. Among various magnetic materials, spinel type iron oxides, such as magnetite (Fe_3O_4) and maghemite (γ-Fe_2O_3), have attracted much attention, especially in the field of bio-applications. Magnetite is an ideal candidate material for biomedical use. It is ferrimagnetic and possesses moderate saturation magnetization [3]. Most of all, it is reported to be biocompatible. However, the magnetite nanoparticles are not stable in oxygen-abundant applications and oxidize to ferric oxi-hydroxides, which have different properties [4]. Rather, maghemite nanoparticles have much better chemical stability along with similar magnetic properties. These properties make maghemite a suitable material for bio-applications, such as magnetic hyperthermia or magnetic resonance image (MRI) contrast agent. In this paper, we report the synthesis of superparamagnetic maghemite nanoparticles and discuss its structural, thermal, and magnetic properties as a basic material for biological applications.

*Corresponding author: Tel: +82-63-469-4562
Fax: +82-63-469-4561, e-mail: shyoon@kunsan.ac.kr

2. Experimental

Nano-sized maghemite particles were synthesized by a chemical co-precipitation method, followed by a temperate oxidation process. Aqueous mixtures of $FeCl_2 \cdot 4H_2O$ and $FeCl_3 \cdot 6H_2O$, with appropriate molar ratios, were first prepared. Then, a NaOH solution was slowly dropped into this solution with vigorous stirring, under the flow of Ar gas. The solution was stirred at 80°C for one hour and turned from red brown to black. The final pH was 11. After adding diluted HCl to neutralize the solution, the resulting black precipitate was gathered by pouring off the supernatant with a strong magnet underneath and subsequently rinsed 4 times with warm water. Transformation from this iron oxide to maghemite was performed by storing the precipitate in a neutral solution and exposing it to the air for several days on the shelf. In order to accelerate the rate of this transformation, an aerating oxidation of acidified aqueous magnetite suspension was previously proposed [5].

The particles were dried overnight under vacuum and used for subsequent measurements. The crystallographic and morphological characterizations were carried out by using x-ray diffraction (XRD) and field emission scanning electron microscopy (FE-SEM), respectively. The variations of the sample weight, with heating, was monitored using thermogravimetric analyses (TGA), up to 900°C, under both air and N_2 atmosphere. Hysteresis

loops and zero-field cooled (ZFC) – field-cooled (FC) magnetization curves were obtained by using a vibrating sample magnetometer (VSM). Mössbauer spectra at various temperatures were collected by using a spectrometer of transmission type with a ^{57}Co source in a rhodium matrix at ambient temperature.

3. Results and Discussion

FE-SEM image in Fig. 1 shows the morphology of the γ-Fe_2O_3 nanoparticles, in which the regular nature of the grain was observed. It was the image for dried powder so it showed some degree of agglomeration. The grain size ranged from 10 to 15 nm. Powder XRD pattern of γ-Fe_2O_3 nanoparticles is shown in Fig. 2. It consisted of peaks for single spinel structure without any other phases. The width of the peaks was broad, indicative of small particle size. The average size (D_{XRD}) of the γ-Fe_2O_3 nanoparticles was determined by using the Debye-Scherrer formula [6]:

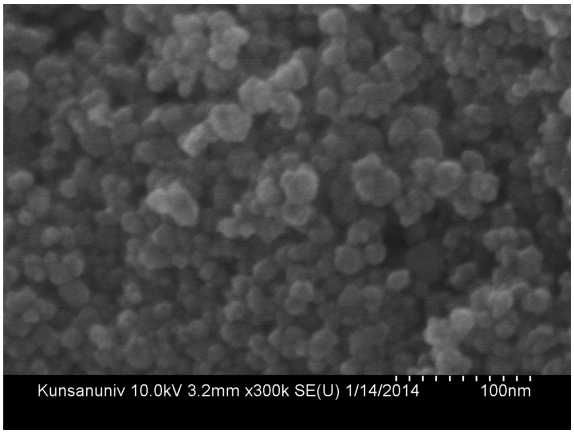

Fig. 1. FE-SEM image of the maghemite nanoparticles.

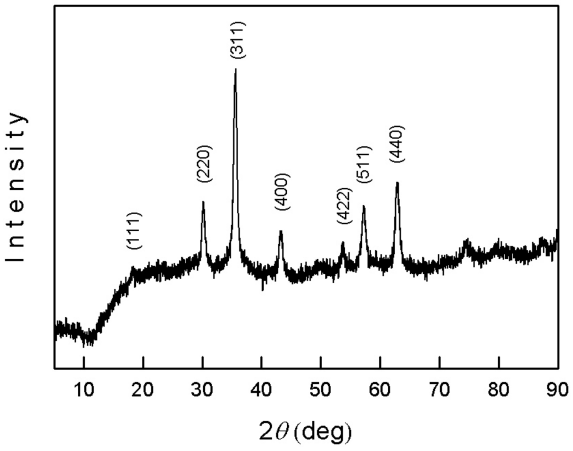

Fig. 2. Powder XRD pattern of the maghemite nanoparticles.

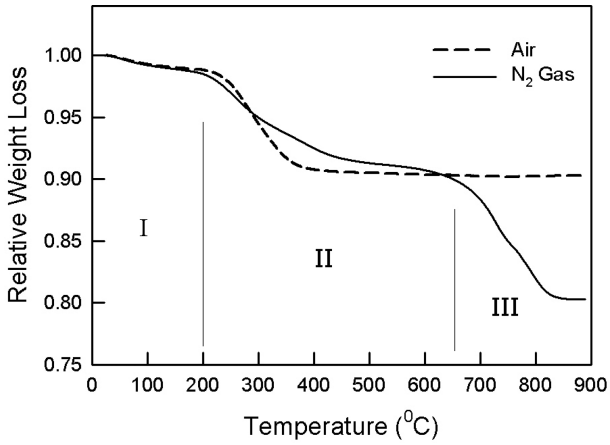

Fig. 3. TGA profiles of the maghemite nanoparticles obtained under air and N_2 gas.

$$D_{XRD} = \frac{0.9\lambda}{\beta\cos\theta} \quad (1)$$

where 0.9 was the Scherrer's constant, λ was the wavelength of the Cu $K\alpha$ radiation ($\lambda = 1.5406$ Å), β was the broadening in the full width at half maximum in radians, and θ denoted the Bragg angle. The value of D_{XRD} was calculated to be 13.9 nm, which fell well within the range observed in the SEM image.

The stages of weight loss with the increase of temperature for the γ-Fe_2O_3 nanoparticles is illustrated in Fig. 3. The first stage (I) was up to 200°C, where the evaporation of absorbed moisture occurred. At the second stage (II), from 200°C to 650°C, 10% of weight loss occurred according to the irreversible reaction of γ-$Fe_2O_3 \rightarrow Fe_2O_3 \rightarrow 2FeO$ [7]. Here, 2FeO phase was meta-stable high temperature phase and returned to hematite as soon as the sample was cooled back [8]. When the sample was further heated under an oxygen-free environment, 2FeO lost one more oxygen atom, resulting in the observed 20% weight loss.

The *M-H* curves for the γ-Fe_2O_3 nanoparticles are depicted in Fig. 4. The curve measured at 300 K showed no hysteresis without any coercivity, which meant the sample was superparamagnetic. The saturation magnetization was 68 emu/g, which was slightly smaller than that for the bulk material (74 emu/g) [9]. At 30 K, the loop exhibited small coercivity ($H_C = 100$ G), as shown in the inset. We got the particle size and its distribution by fitting the hysteresis curve to the classical Langevin function weight-averaged with a particle size distribution function $f(r)$:

$$M(H) = M_S \int_0^\infty L(r, H) f(r) dr \,. \quad (2)$$

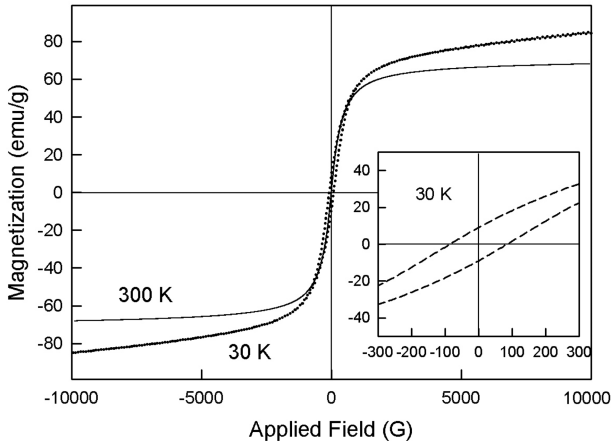

Fig. 4. The *M-H* curves for the maghemite nanoparticles measured at 30 K and room temperature. The inset shows a detailed view for small-field region.

Here, we assumed a modified log-normal particle size distribution $f(r)$ [10]:

$$f(r) = \frac{1}{(r-\theta)\sqrt{2\pi}\sigma} \exp\left[\left(-\ln\frac{r-\theta}{r_0}\right)^2 / 2\sigma^2\right]. \quad (3)$$

Optimum fit was obtained for $\sigma = 0.28$, $r_0 = 4.63$, $\theta = 0.2$, and the result is displayed in Fig. 5. Average particle size D_{MAG} was the first moment of the distribution $f(r)$ and was estimated to be 10.1 nm, which was smaller than D_{XRD} deduced from XRD analysis. For magnetic nanoparticles, the magnetic size was always smaller than that deduced from structural measurements. This fact along with the reduction in saturation magnetization described above came from the core-shell structure of particles and can be explained by the existence of shell layers with the incomplete coordination of atoms on the particle surface,

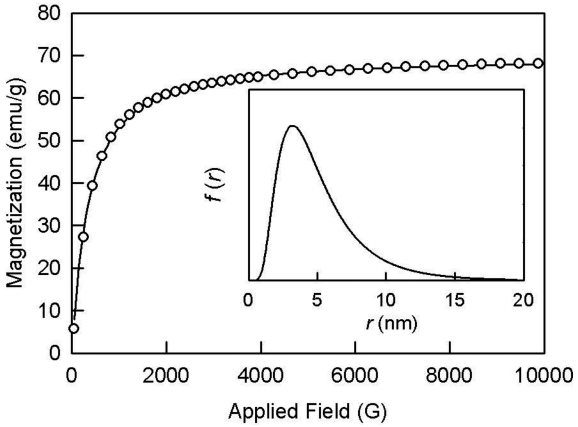

Fig. 5. Results of the *M-H* curve analysis (Eq. (2)) for the maghemite nanoparticles. Corresponding particle size distribution function $f(r)$ is shown in the inset.

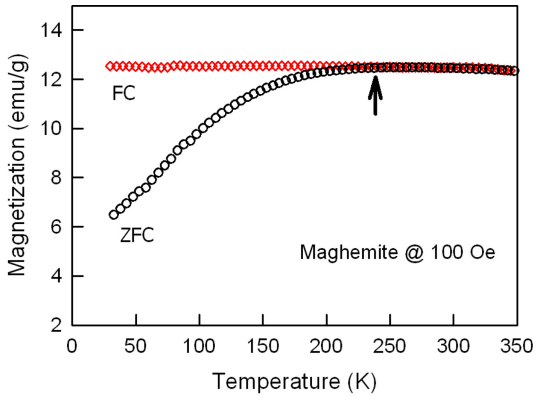

Fig. 6. (Color online) FC and ZFC magnetization curves under 100 Oe for the maghemite nanoparticles. The arrow represents the blocking temperature T_B.

leading to the magnetic dead layer.

Figure 6 shows the FC-ZFC magnetization curves for the γ-Fe_2O_3 nanoparticles taken under 100 Oe. Blocking temperature T_B of a nanoparticle system was usually defined as the bifurcation point of the two curves [11], which was determined, from the figure, to be 240 K for this sample.

Mössbauer spectra taken at various temperatures are illustrated in Fig. 7. As shown in this figure, the Mössbauer absorption lines broaden asymmetrically as the temperature rose, which can be explained by the multiple possible environments of Fe ions. The γ-Fe_2O_3 was known to have the spinel (AB_2O_4) structure in which there were insufficient Fe^{3+} cations to fill all the octahedral (B) and tetrahedral (A) sites so that the stoichiometry corresponded to $Fe_{8/3}\square_{1/3}O_4$ where □ represented a cation vacancy [12]. If

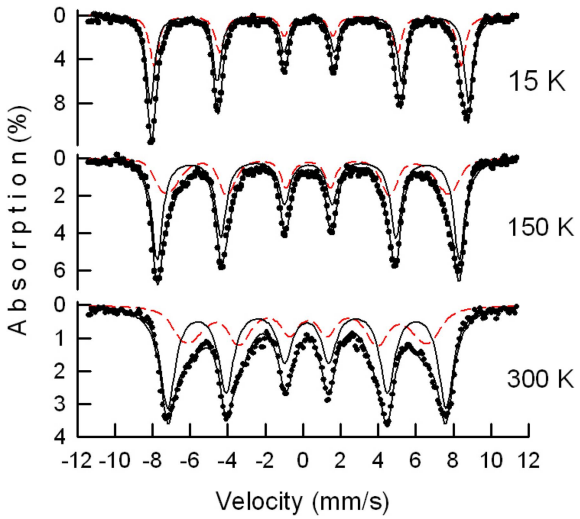

Fig. 7. (Color online) Mössbauer spectra of the maghemite nanoparticles taken at various temperatures. The inner and the outer sets correspond to the A and the B sites, respectively.

all the vacancies were present on the B-sites, the chemical formula would be $Fe_A(Fe_{5/3}\square_{1/3})_BO_4$, implying that an A-site Fe ion was surrounded by 12 B-sites, which can be either an Fe^{3+} ion or a vacancy, while all the B-site Fe ions were only surrounded by 6 A-site Fe ions. The probability for an A-site Fe ion having n Fe ions among 12 neighboring B-sites cavity became

$$P(n) = {}_{12}C_n x^n (1-x)^{12-x}$$

where x was the fraction of vacancies in the B-site. Therefore, the A-site subspectra can be fitted as the superposition of magnetic sextets with hyperfine field of $H(n) = H_0 - (12-n)\Delta H$ and relative absorption intensity of $P(n)$. The H_0 was the A-site hyperfine field with no B-site vacancy neighbors and ΔH was the decrement in hyperfine field, as a result of replacing a B-site Fe neighbor by a cation vacancy. Experimental absorption area ratio A/B was found to be 0.6-0.65 throughout the temperature range examined, which agreed well with the assumption that most of the vacancies resided in B-site. The isomer shift values at room temperature for the A and the B-site were 0.24 mm/s and 0.29 mm/s, respectively, which were typical values for Fe^{3+}.

Interestingly, the sample was paramagnetic at room temperature from VSM measurement while the magnetic hyperfine structure from Mössbauer measurement did not collapse. This result originated from different measuring time scales for the two methods [13]. The measurement time window for Mössbauer spectroscopy (~10^{-9} sec) was extremely narrow, enough to follow up the relaxational fluctuation of magnetic moment. On the other hand, the time scale for VSM measurement (~10 sec) was so long that it could only reflect the averaged value, i.e., the vanishing magnetic moment.

4. Conclusion

Maghemite nanoparticles have been prepared by the chemical co-precipitation, followed by a mild oxidation process, and subjected to various physical characterizations. The synthesized nanoparticles were typically 13.9 nm in size and proved to be pure maghemite or $Fe_A(Fe_{5/3}\square_{1/3})_BO_4$ without the contamination from any other forms of iron oxide. The results of the investigations indicated that the synthesized maghemite nanoparticles possessed all the required physical properties necessary for bio-applications, such as magnetic hyperthermia treatment or MRI contrast agent.

Acknowledgment

This work was supported by the Basic Science Research Program (2010-0023413) thru NRF of Korea.

References

[1] K. M. Krishnan, IEEE Trans. Magn. **46**, 2523 (2010).
[2] Q. A. Pankhurst, J. Connolly, S. K. Jones, and J. Dobson, J. Phys. D: Appl. Phys. **36**, R167 (2003).
[3] M. Gonzales and K. M. Krishnan, J. Magn. Magn. Mater. **293**, 265 (2005).
[4] Y.-K. Sun, M. Ma, Y. Zhang, and N. Gu, Colloid Surf. A: Physicochem. Eng. Aspects **245**, 15 (2004).
[5] Y. S. Kang, S. Risbud, J. F. Rabolt, and P. Stroeve, Chem. Mater. **8**, 2209 (1996).
[6] B. D. Cullity, Elements of X-Ray Diffraction, Addison-Wesley, Reading (1975).
[7] C. A. Jacobson, Encyclopedia of Chemical Reactions vol. IV, Reinhold Publishing Co., New York (1951) p. 110.
[8] J. Fang, A. Kumbhar, W. L. Zhou, and K. L. Stokes, Mat. Res. Bull. **38**, 461 (2003).
[9] E. P. Wohlfarth, Ferromagnetic Materials vol.2, North-Holland Publishing Co., Amsterdam (1980) pp. 430-431.
[10] Sunghyun Yoon and K. M. Krishnan, J. Appl. Phys. **109**, 07B534 (2011).
[11] T. Hyeon, Y. Chung, J. Park, S. S. Lee, Y.-W. Kim, and B. H. Park, J. Phys. Chem. B **106**, 6831 (2002).
[12] N. N. Greenwood and T. C. Gibb, Mössbauer Spectroscopy, Chapman and Hall Ltd., London (1971).
[13] C. Cannas, A. Musinu, G. Piccaluga, D. Fiorani, D. Peddis, H. K. Rasmussen, and S. Mørup, J. Chem. Phys. **125**, 164714 (2006).